Nonmonotonic dependence of thermal conductivity on surface roughness: A multiparticle Lorentz gas model

Tingting Wang, Shuang Tian, Dengke Ma,* and Lifa Zhang†

Phonon Engineering Research Center of Jiangsu Province, Center for Quantum Transport and Thermal Energy Science, Institute of Physics Frontiers and Interdisciplinary Sciences, School of Physics and Technology, Nanjing Normal University, Nanjing 210023, China

(Received 20 December 2022; revised 4 April 2023; accepted 27 June 2023; published 24 July 2023)

Utilizing surface roughness to manipulate thermal transport has aided important developments in thermoelectrics and heat dissipation in microelectronics. In this paper, through a multiparticle Lorentz gas model, it is found that thermal conductivity oscillates with the increase of surface roughness, and the oscillating thermal conductivity gradually disappears with the increase of nonlinearity. The transmittance analyses reveal that the oscillating thermal conductivity is caused by localized particles due to boundary effects. Nonlinearity will gradually break the localization. Thus, localization still exists in the weak nonlinear system, where there exists an interplay between nonlinear interaction and localization. Furthermore, it is also found that boundary shapes have a great influence on the oscillating thermal conductivity. Finally, we have also studied the oscillating thermal rectification effects caused by rough boundaries. This study gains insight into the boundary effect on thermal transport and provides a mechanism to manipulate thermal conductivity.

DOI: 10.1103/PhysRevE.108.014125

I. INTRODUCTION

With the continuous progress of nanotechnology, the length scale of integrated circuits is rigorously reduced to nanometers. Heat dissipation becomes a serious problem to avoid overheating of microelectronic and other quantum devices [1,2]. To facilitate heat dissipation, increasing the thermal conductivity of materials is a good strategy [3,4]. At the same time, thermoelectric technology, which converts waste heat directly into electrical energy, can benefit from the decrease in thermal conductivity of materials [5–7]. Thus, exploring strategies to manipulate thermal conductivity of materials is of vital importance. It has been shown that thermal conductivity is highly dependent on the shape, size, and boundary conditions of material at nanoscale [8–12] due to the fact that surface roughness is an inevitable characteristic of nanomaterials, which can be easily modulated [13,14]. Utilizing boundary scattering to manipulate thermal conductivity has attracted tremendous attention [15,16].

Many experiments and theoretical models have been developed to study the effect of rough boundary on thermal conductivity [14,17–21]. Theoretical research points out that rough boundaries will induce diffusive phonon scattering, resulting in a decrease in thermal conductivity [14,17,20,22]. Simulations and experiments on real materials, for example, silicon nanowires [16,23,24] and graphene nanoribbon [17,25], all demonstrate the above point. On the one hand, an obvious decrease in thermal conductivity has been observed in the presence of surface roughness. On the other hand, the thermal conductivity will further decrease as the surface roughness increases [16]. Except particle-based scattering, when the wave-based phonon interference happens at rough surface, thermal conductivity can be reduced more strongly [15,19]. Although previous studies have shown that thermal conductivity decreases with the increase of surface roughness, recent study has shown that thermal conductivity oscillates with surface roughness [26]. This is different from the effects of rough boundaries as we knew before and implies that, within a specific range, thermal conductivity can be enhanced by increasing surface roughness. This phenomenon holds great promise for the regulation of thermal conductivity, and it is therefore worth investigating the underlying mechanisms.

However, previous research has focused solely on linear systems [26], where there are no many-body interactions and localization occurs [27]. Naturally, we pose the question: Is localization the underlying mechanism, considering that real materials have both linear and nonlinear interactions, and the latter will destroy phonon coherence and localization [28–30]? It is worthwhile to explicitly elucidate the underlying mechanism and explore the effect of nonlinearity on oscillating thermal conductivity. At the same time, it is also important to reveal the effect of rough boundary shape on oscillating thermal conductivity. This will aid the design of materials to utilize the oscillating thermal conductivity for heat dissipation or thermometrics.

In this paper the multiparticle Lorentz gas model (LGM) is used to investigate thermal transport in two-dimensional ribbons with rough surfaces. The collision probability (P) is used to measure the nonlinear interactions. First, the dependence of thermal conductivity on surface roughness for systems with different nonlinear interactions is studied. Then the transmittance (τ) for particles at different emitted angles (θ) is calculated and compared for the peak and valley of

*dkma@njnu.edu.cn
†phyzlf@njnu.edu.cn

oscillating thermal conductivity to clearly show localization and reveal the underlying mechanism. The dependencies of oscillating thermal conductivity on system width and the shape of rough surfaces are also studied. Finally, we have also explored the oscillating thermal rectification effects caused by rough boundaries.

II. MODELS

A. Multiparticle LGM

The multiparticle LGM, developed from LGM [31–34], is used to simulate thermal transport in different systems. In general, the LGM involves particles moving in a field of fixed scatterers, either periodic or random, with the particles either reflecting off the scatterers (hard core model) or being pushed apart by the potential (soft core model). This traditional LGM is a quasi-one-dimensional model by simulating the particle behavior after a single particle collides with media added in space. In this case it has been found that rough boundaries can be substituted for internally placed scatterers to form temperature gradients [26]. It is thought that phonon-phonon interactions play an important role in heat transport [2,28,35,36]; therefore we considered the phonon-phonon interactions and developed traditional LGM into a two-dimensional multiparticle LGM [11,12].

In our multiparticle LGM, the temperature field is formed by adding high and low temperatures at both ends of the structure, and a large number of particles are placed as heat carriers. When a particle hits the left and right ends, it is absorbed by the heat source, and then is reemitted according to the temperature of the heat source, following the Maxwell velocity distribution [Eqs. (1) and (2)] [34]. Here v_x and v_y are the x- and y-axis components of a particle's velocity. Both the upper and lower boundaries are adiabatic. The heat flow (J) can be obtained by counting the heat absorption and release of a heat source in the steady state as in Eq. (3). By dividing the model into multiple regions, the sum of kinetic energy of particles in each region can be counted. Then the temperature distribution in the model can be obtained as in Eq. (4). After getting the temperature distribution and heat flow, Eq. (5) can be used to calculate the overall thermal conductivity of the model. Here ΔT is the temperature difference between the left and right sides:

$$P(v_x) = \frac{|v_x|}{T} \exp\left(-\frac{v_x^2}{2T}\right), \tag{1}$$

$$P(v_y) = \frac{1}{\sqrt{2\pi T}} \exp\left(-\frac{v_y^2}{2T}\right), \tag{2}$$

$$J = \frac{\Delta E}{\Delta t}, \quad E = E_{\text{released}} - E_{\text{absorbed}}, \tag{3}$$

$$T(x) = \frac{E(x)}{k_B}, \tag{4}$$

$$\kappa = \frac{Jl}{d\Delta T}. \tag{5}$$

In this model phonon-phonon interactions are simulated by probabilistic collisions between particles. Close particles collide according to collision probability (P). When $P = 0$, there is no collision between particles, simulating ballistic transport, and the nonlinearity of the system is zero. Thus, by increasing P from zero, the modeled system can be transformed from linear to nonlinear conditions. A more detailed discussion of the relationship between P and nonlinearity is presented in the next section. Compared to commonly used molecular dynamics simulations [2] and the atomic Green's function method [37], this model can simulate the intermediate process from ballistics to diffusion.

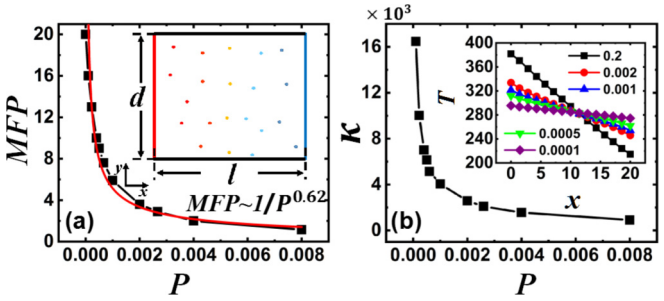

FIG. 1. (a) The change in mean-free-path (MFP) with the collision probability (P). Inset: Schematic diagram of the rectangular multiparticle Lorentz gas model (LGM). (b) The change in thermal conductivity (κ) with the collision probability (P). Inset: The temperature distribution varies with P.

Our model provides an alternative approach to studying heat transport. On the one hand, by varying the overall nonlinearity and boundary shape of the model, the effect of nonlinearity (transition from ballistic to diffusive transport) and boundary shape on thermal conductivity and thermal rectification effects can be investigated [11,12]. On the other hand, we can also simulate heat transport in the case of heterojunctions by varying the particle number density to change the material class and by varying the nonlinearity in a region. Therefore, we believe that simulations using our model for different heat transport scenarios can deepen the understanding of heat transport mechanisms and facilitate the discovery of new phenomena.

B. Nonlinearity and collision probability

To demonstrate that a change in P can correspond to a change in nonlinearity, we focus on the temperature gradient, thermal conductivity, and mean-free-path (MFP) for a rectangular structure. The schematic diagram of the modeled rectangular structure is shown in the inset of Fig. 1(a). The length of the rectangle is l, and the width is d. The heat source of T_1 and heat sink of T_2 are placed on the left and right sides. The collisions between particles and boundaries are treated as mirror reflections. Throughout this paper, T_1 and T_2 are fixed at 400 and 200, respectively. At this time, $l = 20$ and $d = 10$, and the particle number density in the model is 11 particles per unit area.

Since it has been proved that the thermal conductivity in the lattice is inversely proportional to the nonlinearity [38], in order to further illustrate that P can represent the nonlinearity, we calculate the trend of the thermal conductivity in the model with P, as shown in Fig. 1(b). It can be obtained by fitting that $\kappa \propto P^{-0.62}$. The inset of Fig. 1(b) shows the temperature distribution as P increases from 10^{-4} to 0.2. It can be observed

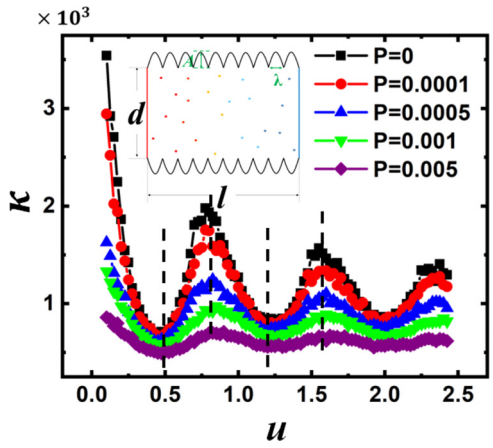

FIG. 2. Variation of thermal conductivity (κ) with roughness (u) under different nonlinearities. Inset: Schematic diagram of rough boundary model of trigonometric function.

that the temperature gradient is quite small when $P = 10^{-4}$. This is in accordance to the conditions when the nonlinearity of the model is weak. When P increases, the nonlinearity increases, and temperature gradient increases. Obviously, the strong and weak relationship of nonlinearity in the model is associated with P, so that P could be used as a measure of nonlinearity of the following models.

More directly, nonlinearity can induce high-order scattering and affect relaxation time as well as MFP. These points have been widely demonstrated and accepted [38–40]. To show more clearly that a change in P can correspond to a change in nonlinearity, the MFPs of particles for the same rectangular structure are calculated and shown in Fig. 1(a) with different P. It can be observed that MFP decreases with the increase in P. As temperature stays the same here, the group velocity does not change. The decrease of MFP is due to the decrease of relaxation time. This comes from the increase of nonlinearity, which increases the probability of particle collisions. More precisely, MFP$\propto P^{-0.62}$, which shares the same rule with previous studies that MFP is inversely proportional to the nonlinearity [38]. These further confirm that P can correspond to nonlinearity.

C. Rough boundary model

In the following section, rough boundaries are introduced to study the effect of the boundary on thermal transport. The upper and lower boundaries of the structure are changed to the same sinusoidal (see the inset of Fig. 2), hyperbolic tangent, and rectangular [see the inset of Fig. 5(a)] shapes. In these structures, the amplitude of boundary is A, and the periodic length is λ. The roughness of boundary is defined as $u = \frac{A}{\lambda}$ [26]. In this paper, since thermal conductivity is not directly related to A and λ but to u [26], we can change u by changing A while keeping λ constant as 4. The hyperbolic tangent boundary can be expressed as Eq. (6). When the coefficient b is equal to 1, the hyperbolic tangent boundary is closer to the shape of the sinusoidal function, and as b increases, the hyperbolic tangent boundary becomes closer to the rectangular case. The rectangular boundary is formed on the hyperbolic tangent boundary of $b = 4$, looking only at the shape of the boundary, the part where amplitude greater than 96% of A is set to the upper edge of the rectangle, and the part less than 96% of A is set to the lower edge. Considering the size of upper and lower boundaries, the average velocity of particles, and the step length, l and d are set to 200 in the following, and the particle number density is set to 0.05 particles per area. All parameters used in this model are dimensionless:

$$\begin{cases} y = A\tanh(bx_n), & 0 \leqslant x_n \leqslant \frac{\lambda}{2} \\ y = A|\tanh[b(x_n - \lambda)]|, & \frac{\lambda}{2} < x_n < \lambda \\ x_n = x - \lfloor \frac{x}{\lambda} \rfloor \lambda. \end{cases} \tag{6}$$

III. OSCILLATING THERMAL CONDUCTIVITY DUE TO BOUNDARY EFFECTS

To explore the effect of nonlinearity interactions, thermal conductivities for systems with sinusoidal boundaries are calculated and shown in Fig. 2 for five different nonlinearities. It can be observed that for a linear system ($P = 0$), the thermal conductivity oscillates apparently with increasing surface roughness, which is consistent with the results of previous work simulated by single-particle LGM [26]. This further illustrates the correctness of our multiparticle LGM. Then, as P increases, nonlinearity increases and the amplitude of thermal conductivity oscillation decreases. This implies that thermal conductivity oscillation is sensitive to nonlinear interactions, and nonlinearity can weaken oscillation. It can be seen from Fig. 2 that, when roughness is smaller than 0.5, the thermal conductivity decreases more slowly for a system with larger nonlinearity. This means that the boundary effect diminishes. When $P = 0.005$, the oscillation of thermal conductivity is still present but very weak. It can be inferred that the thermal conductivity oscillation will eventually disappear as the nonlinearity continues to increase.

It should be emphasized that this is not a simple point about the effect of the boundary or nonlinearity on thermal conductivity. Rather, it is an elaboration about the effect of nonlinearity on localization induced by rough boundaries. This issue of how nonlinearity affects localization has been a matter of widespread interest, for example, in the case of Anderson localization caused by multiple scattering in disordered systems [41]. Some studies show that arbitrary nonlinearity can destroy the Anderson localization [42]. Some studies have suggested the existence of a threshold in the interaction strength of nonlinearity [43] below which localization remains. Here we clearly show that nonlinearity weakens localization gradually, as oscillating thermal conductivity still exists in the weak nonlinear system. If arbitrarily small nonlinearities can destroy the localization caused by rough boundaries, the oscillation of thermal conductivity will suddenly disappear. This will also shed light in future studies that oscillating thermal conductivity may also exist in real materials with weak nonlinearity or at low temperature.

To explore the underlying mechanism of thermal conductivity oscillation, the transmittance (τ) of particles emitted at different angles (θ) from the heat source is calculated. Here, due to the symmetry of the modeled structure, the θ

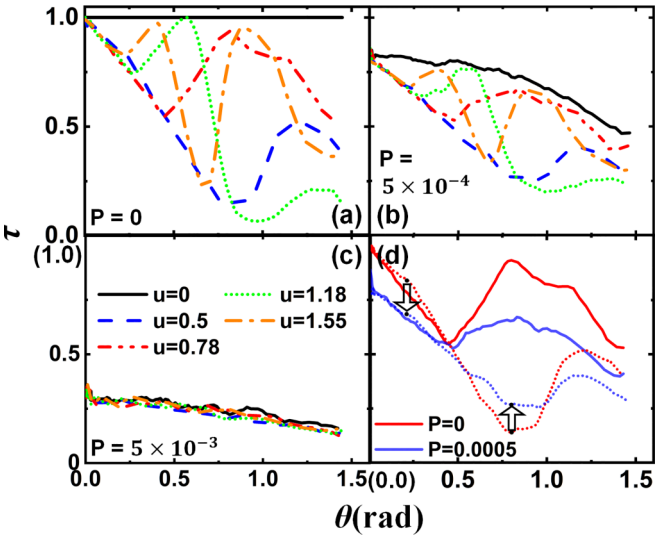

FIG. 3. (a)–(c) The relationship between the emitted angle [θ(rad)] and transmittance of particles (τ) under different nonlinearities (P). (d) The relationship between τ and θ for two cases of nonlinearity ranging from small to large; here $u = 0.5$ (dashed line) and 0.78 (solid line).

of each particle is defined as $\theta = |\text{atan}(\frac{v_y}{v_x})|$. The τ is denoted as 1(0) if the particle can(not) reach the heat sink from the heat source. The τ of each θ is calculated by averaging over 200 particles emitted at the same angle. To capture the main difference, we focus on the peaks and valleys of oscillating thermal conductivity shown in Fig. 2 and choose five points with $u = 0, 0.5, 0.78, 1.18$, and 1.55. The θ-dependent τ of particles for the four structures are calculated and compared with others for cases with different nonlinear interactions.

The θ-dependent τ for different systems is shown in Fig. 3. For the purely linear structures, as shown in Fig. 3(a), the τ is always equal to 1 no matter how the θ changes when $u = 0$. This is in accordance with related studies about ballistic transport [26]. When the roughness of boundaries increases, the τ for four cases with $u = 0.5, 0.78, 1.18$, and 1.55 are much lower than that of $u = 0$ in the whole θ range. This shows that the introduction of rough boundaries reduces particle transport and therefore thermal conductivity. More importantly, if we focus on the oscillating peaks [$u = 0.78$ and 1.55 in Fig. 3(a)] and valleys [$u = 0.5$ and 1.18 in Fig. 3(a)], large differences can be observed. For the two oscillating valleys, particles emitted between 0.78 (45°) and 1.31 (75°) have low τ. However, within the above same θ, for the two oscillating peaks, the τ ranges from 0.75 to 1, which is much higher than 0.5. The τ of oscillating peaks and valleys are almost the same at small θ. This is because most of these particles are ballistically transported through the system. When θ increases, especially between 0.78 (45°) and 1.31 (75°), the τ of the oscillating peaks and valleys are quite different. This difference becomes small again when the θ is large. The reduction of the τ in the valley case is because of the localization in the system (details are explained later). The less rough case happens to have more particles localized at the boundary. When the roughness increases, the localization is weakened, and the transmission is enhanced. Then we compared the two peaks, and it can be found that the thermal conductivity of the second peak is lower than that of the first, and this is due to the second peak corresponding to a very small τ when θ is 0.75 (43°), meaning that there is still a fraction of phonons that undergo strong localization. From this we see that the oscillations in thermal conductivity caused by rough boundaries are due to the different effects of the boundary on the transmittance of particles for different roughness. This provides insights into the boundary effect on the thermal transport.

When nonlinearity is introduced, τ for the same structures are shown in Figs. 3(b) and 3(c). For the structure with $u = 0$, the increase in nonlinearity leads to an overall decrease in τ, which is consistent with the fact that nonlinear scattering hinders thermal transport [20]. For structures with different boundary roughness, it can be found that their differences in τ become smaller when P increases from 0.0005 to 0.005. When the nonlinearity is large enough, for example, $P = 0.005$, τ of the five structures become nearly equal. This is in accordance with the weakly oscillating thermal conductivity shown in Fig. 2. At this point, particle transport is mainly governed by interparticle interactions, and the effect of the boundary can be negligible.

More interestingly, the change in τ is quite different between oscillating peak and valley structures when nonlinearity (P) increases. To better illustrate this point and the effect of nonlinearity, Fig. 3(d) picks the τ of the oscillating peak ($u = 0.78$) and valley ($u = 0.5$) with nonlinearity of 0 and 0.0005. For the oscillating peak, as shown by the solid line in Fig. 3(d), there is an overall decrease in τ in the whole θ range when P increases from 0 [red (dark-gray) solid line in Fig. 3(d)] and 0.0005 [blue (light-gray) solid line in Fig. 3(d)]. For the oscillating valley, with a smaller θ, there is also an overall decrease in τ at a certain range from 0 (0°) to 0.52 (30°). This is mainly due to the hindering effect of nonlinearity on transport. An unusual increase in τ occurs at a certain θ range from 0.78 (45°) to 1.05 (60°), where the localization originally occurs and results in the lower thermal conductivity of structure with smaller roughness of boundary. This is because the nonlinearity disrupts localization and enhances this part of the particle transport. This anomalous change in τ indicates that there exists an interplay between nonlinear interaction and localization in nonlinear system. It is for these reasons that the initial localization gradually diminishes and the oscillation gradually becomes smaller when P increases. This further supports our understanding of the mechanisms underlying the effect of boundary effects on heat transport and provides a mechanism for future manipulation of thermal conductivity.

It is determined that the increase of nonlinearity makes the thermal conductivity decrease with the amplitude of the roughness oscillation while the period remains unchanged, as shown in Fig. 2, which is due to the weakening of the localization caused by the boundary effect. We think that the distance between the upper and lower rough boundaries, that is, the width of the structure (d), may influence the oscillation period [44]. We then changed the width of the structure for four different cases. Here $P = 0$, which means this is a linear structure. Marking the distance between the point of zero roughness and the first valley point of thermal conductivity as 1, and the distance between first valley and first peak as 2,

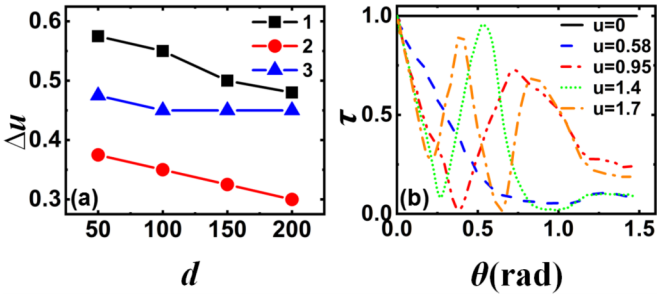

FIG. 4. (a) The period of oscillation (Δu) varies with width (d) in the case of three different peaks and valleys, here $P = 0$. (b) The relationship between the emitted angle [θ(rad)] and transmittance (τ) of particles, here $d = 50$.

then the distance between the first peak and the second valley as 3, we could obtain the relationship between d and period of the oscillation (Δu), as shown in Fig. 4(a).

It can be seen that the periods of oscillation decrease as the width increases. The θ-dependent τ for a structure with a width of 50 is shown in Fig. 4(b). Compared with Fig. 3(a), it is found that the overall trend is about the same. When $u = 0$, τ is always 1 for the same reason, but θ is different where the difference is largest. For example, the red line representing the first peak of the oscillation reaches its highest value when θ is between 0.59 (36°) and 0.78 (45°) in Fig. 3(a). However, it's 0.69 (40°) and 0.88 (50°) in Fig. 4(b). This shows that changing the width affects the scattering direction of particles.

After obtaining the factor of width which affects the period, it is considered that oscillating thermal conductivity has not been observed in previous studies on the rectangular rough boundary model [20]. Whether the boundary shape has an effect on the oscillation of thermal conductivity remains to be studied. We then changed the rough boundary to a hyperbolic tangent shape, as shown in the inset of Fig. 5, and its expression can be found in the previous section. We changed the coefficient b of the four sets of hyperbolic tangent functions. Then we also added a rectangular boundary model to Fig. 5. It can be seen that the thermal conductivity still oscillates with roughness when the hyperbolic tangent coefficient (b)

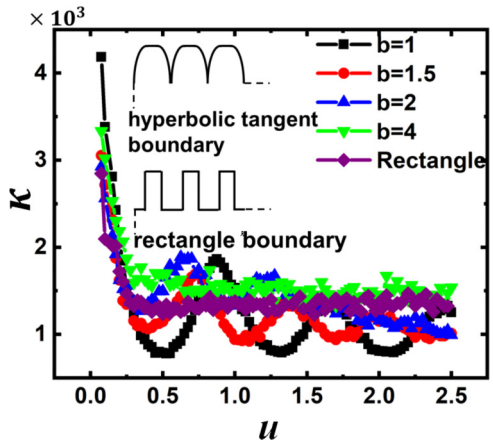

FIG. 5. The thermal conductivity (κ) varies with roughness (u) under different boundary shapes. Inset: Schematic diagram of different boundary shapes.

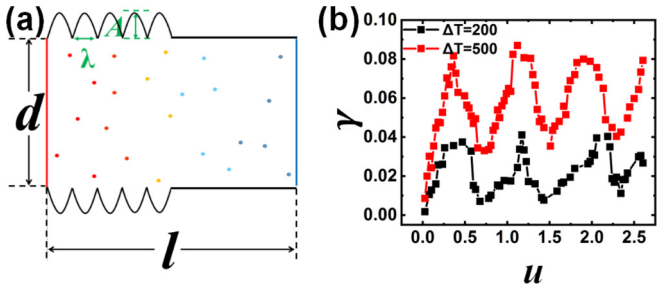

FIG. 6. (a) Diagram of the semirough and semirectangular model. (b) The dependence of the thermal rectification ratio (γ) on roughness (u) at different temperature differences (ΔT).

is increasing by a relatively small amount. Only the period and amplitude of the oscillation are gradually decreasing. When $b = 4$, the oscillation disappears after two cycles. In the rectangular case, the oscillation disappears completely. This indicates that keeping the boundary smooth is conducive to the localization of particle collisions at the boundary, leading to the oscillation effect.

This further verifies that the oscillations of thermal conductivity are due to localization caused by boundary effects, and the localization is determined by the different scattering direction of particles with different emitted angles, which is caused by different rough boundaries. In the case of a smooth sinusoidal-like boundary ($b = 1$ in Fig. 5), the τ of particles with different θ differ significantly, similar to the case in Fig. 3. In contrast, in the case of a rectangular boundary, the scattering direction of the particles does not change significantly with increasing roughness. Thus, the τ of the particles with different emitted angles do not differ much either, so that the thermal conductivity of the rectangular boundary does not oscillate. The different boundary shapes have different abilities to induce oscillating thermal conductivity, which not only explains the previous inability to observe oscillating thermal conductivity at rectangular rough boundaries, but also provides guidance for the future use of rough boundaries to modulate thermal conductivity.

IV. OSCILLATING THERMAL RECTIFICATION EFFECTS

The regulation of the thermal rectification ratio by changing the boundary shape has been explored before by multiparticle LGM [11,12]. However, whether rough boundaries cause thermal rectification effects is still an open question which would guide the design of thermal devices, such as thermal diodes [8]. Therefore, we focus on a semirough and semirectangular structure shown in Fig. 6(a) and explore the thermal rectification effect therein. The parameter, the thermal rectification ratio, which measures the strength of the thermal rectification effect is defined as $\gamma = |\frac{J_+ - J_-}{J_+ + J_-}|$, where J_+ indicates the forward heat flow when the high-temperature heat source is at the left end and J_- indicates the reverse heat flow when the low-temperature heat source is at the left end. Both J_+ and J_- are scalar quantities that characterize the magnitude of the heat flow. The length (l) and width (d) of this model are the same as the rough boundary models above, while the rough boundary period (λ) is changed to 3.84. The

temperature difference between the left end and right end is ΔT.

The thermal rectification ratio at different boundary roughness is shown in Fig. 6(b). The black line in Fig. 6(b) corresponds to high temperature and low temperature of 400 and 200, respectively, while the red line changes the high temperature and low temperature to 600 and 100, respectively. It can be seen that the overall γ at $\Delta T = 500$ is larger than that at $\Delta T = 200$, suggesting that increasing the temperature difference enhances the thermal rectification effect and makes the trend more pronounced. More importantly, it can be found that γ oscillates as the roughness of the left end of the model increases and is the same as the oscillation period of Fig. 2. This phenomenon can be well explained by the previous conclusion, due to the different scattering of particles at different emitted angles by boundaries of different roughness. In some specific roughness cases where the transmittance of some of the emitted angles is small, and since the right end of the model is rectangular, there is a large difference in the transmittance of the particles at the two ends, which subsequently leads to oscillations where some of the larger γ occur. This further validates the accuracy of our results and also has great application to the adjustment of thermal rectification effects by means of rough boundaries.

V. CONCLUSION

In general, the origin and effect of nonlinearity on oscillating thermal conductivity are studied using the multiparticle Lorentz gas model (LGM). Significant oscillating thermal conductivity has been found in both linear and weakly nonlinear systems. The emitted-angle-dependent transmittance of particle reveals that the oscillating thermal conductivity is due to the localization of particles with different emitted angles, which is caused by different boundary roughness. Increasing nonlinearity reduces the transmittance of nonlocalizing particles, while it also increases the transmittance of localizing particles, so that the difference can be gradually narrowed. This is directly reflected in that the oscillating amplitude of thermal conductivity decreases with the increase of nonlinearity, and nonlinearity can gradually destroy the localization of particles gradually. Therefore, localization still exists in the weak nonlinear system, and there is an interplay between nonlinear interaction and localization in nonlinear system. This can be directly observed in the transmittance of particles. It is also found that the oscillation period can be changed by changing the width of the system and the shape of the boundary. The oscillation can be destroyed by the rectangular boundary, which indicates that boundary shapes have a great influence on particle localization. Finally, we have also explored the oscillating thermal rectification effects caused by rough boundaries. The studies here can deepen the understanding of the effect of nonlinearity and boundary shape on thermal transport.

ACKNOWLEDGMENTS

L.Z. is sponsored by National Natural Science Foundation of China (Grant No. 11975125). D.M. is sponsored by National Natural Science Foundation of China (Grant No. 12005105). T.W. is sponsored by the Postgraduate Research & Practice Innovation Program of Jiangsu Province (Grant No. KYCX23_1677).

The authors declare no competing financial interests.

[1] W. Lee, K. Kim, W. Jeong, L. A. Zotti, F. Pauly, J. C. Cuevas, and P. Reddy, Heat dissipation in atomic-scale junctions, Nature (London) **498**, 209 (2013).

[2] D. G. Cahill, P. V. Braun, G. Chen, D. R. Clarke, S. Fan, K. E. Goodson, P. Keblinski, W. P. King, G. D. Mahan, and A. Majumdar, Nanoscale thermal transport. II. 2003–2012, Appl. Phys. Rev. **1**, 011305 (2014).

[3] X. Xu, J. Chen, J. Zhou, and B. Li, Thermal conductivity of polymers and their nanocomposites, Adv. Mater. **30**, 1705544 (2018).

[4] V. Singh, T. L. Bougher, A. Weathers, Y. Cai, K. Bi, M. T. Pettes, S. A. McMenamin, W. Lv, D. P. Resler, T. R. Gattuso *et al.*, High thermal conductivity of chain-oriented amorphous polythiophene, Nat. Nanotechnol. **9**, 384 (2014).

[5] Z. Jin, Q. Liao, H. Fang, Z. Liu, W. Liu, Z. Ding, T. Luo, and N. Yang, A revisit to high thermoelectric performance of single-layer MoS_2, Sci. Rep. **5**, 18342 (2015).

[6] G. Joshi, T. Dahal, S. Chen, H. Wang, J. Shiomi, G. Chen, and Z. Ren, Enhancement of thermoelectric figure-of-merit at low temperatures by titanium substitution for hafnium in *n*-type half-Heuslers $Hf_{0.75-x}Ti_xZr_{0.25}NiSn_{0.99}Sb_{0.01}$, Nano Energy **2**, 82 (2013).

[7] S. Ju, T. Shiga, L. Feng, Z. Hou, K. Tsuda, and J. Shiomi, Designing Nanostructures for Phonon Transport via Bayesian Optimization, Phys. Rev. X **7**, 021024 (2017).

[8] N. Yang, G. Zhang, and B. Li, Thermal rectification in asymmetric graphene ribbons, Appl. Phys. Lett. **95**, 033107 (2009).

[9] Y. Wang, A. Vallabhaneni, J. Hu, B. Qiu, Y. P. Chen, and X. Ruan, Phonon lateral confinement enables thermal rectification in asymmetric single-material nanostructures, Nano Lett. **14**, 592 (2014).

[10] D. Q. Tran, R. Delgado-Carrascon, J. F. Muth, T. Paskova, M. Nawaz, V. Darakchieva, and P. P. Paskov, Phonon-boundary scattering and thermal transport in $Al_xGa_{1-x}N$: Effect of layer thickness, Appl. Phys. Lett. **117**, 252102 (2020).

[11] T. Wang, Y. Yang, Y. Wu, L. Xu, D. Ma, and L. Zhang, Interface thermal resistance induced by geometric shape mismatch: A multiparticle Lorentz gas model, Phys. Rev. E **104**, 024801 (2021).

[12] H. Wang, Y. Yang, H. Chen, N. Li, and L. Zhang, Thermal rectification induced by geometrical asymmetry: A two-dimensional multiparticle Lorentz gas model, Phys. Rev. E **99**, 062111 (2019).

[13] E. Stratakis, Nanomaterials by ultrafast laser processing of surfaces, Sci. Adv. Mater. **4**, 407 (2012).

[14] B. Qiu, L. Sun, and X. Ruan, Lattice thermal conductivity reduction in Bi_2Te_3 quantum wires with smooth and rough surfaces: A molecular dynamics study, Phys. Rev. B **83**, 035312 (2011).

[15] P. Martin, Z. Aksamija, E. Pop, and U. Ravaioli, Impact of Phonon-Surface Roughness Scattering on Thermal Conductivity of Thin Si Nanowires, Phys. Rev. Lett. **102**, 125503 (2009).

[16] J. Lim, K. Hippalgaonkar, S. C. Andrews, A. Majumdar, and P. Yang, Quantifying surface roughness effects on phonon transport in silicon nanowires, Nano Lett. **12**, 2475 (2012).

[17] D. A. Areshkin, D. Gunlycke, and C. T. White, Ballistic transport in graphene nanostrips in the presence of disorder: Importance of edge effects, Nano Lett. **7**, 204 (2007).

[18] A. S. Mayorov, R. V. Gorbachev, S. V. Morozov, L. Britnell, R. Jalil, L. A. Ponomarenko, P. Blake, K. S. Novoselov, K. Watanabe, T. Taniguchi *et al.*, Micrometer-scale ballistic transport in encapsulated graphene at room temperature, Nano Lett. **11**, 2396 (2011).

[19] J. Sadhu and S. Sinha, Room-temperature phonon boundary scattering below the Casimir limit, Phys. Rev. B **84**, 115450 (2011).

[20] D. Ma, X. Wan, and N. Yang, Unexpected thermal conductivity enhancement in pillared graphene nanoribbon with isotopic resonance, Phys. Rev. B **98**, 245420 (2018).

[21] P. N. Martin, Z. Aksamija, E. Pop, and U. Ravaioli, Reduced thermal conductivity in nanoengineered rough Ge and GaAs nanowires, Nano Lett. **10**, 1120 (2010).

[22] P. E. Hopkins, Thermal transport across solid interfaces with nanoscale imperfections: Effects of roughness, disorder, dislocations, and bonding on thermal boundary conductance, ISRN Mech. Engr. **2013**, 682586 (2013).

[23] A. I. Hochbaum, R. Chen, R. D. Delgado, W. Liang, E. C. Garnett, M. Najarian, A. Majumdar, and P. Yang, Enhanced thermoelectric performance of rough silicon nanowires, Nature (London) **451**, 163 (2008).

[24] E. B. Ramayya, L. N. Maurer, A. H. Davoody, and I. Knezevic, Thermoelectric properties of ultrathin silicon nanowires, Phys. Rev. B **86**, 115328 (2012).

[25] Z. Aksamija and I. Knezevic, Thermal transport in graphene nanoribbons supported on SiO_2, Phys. Rev. B **86**, 165426 (2012).

[26] H. Chen, H. Wang, Y. Yang, N. Li, and L. Zhang, Rough boundary effect in thermal transport: A Lorentz gas model, Phys. Rev. E **98**, 032131 (2018).

[27] H. Matsuda and K. Ishii, Localization of normal modes and energy transport in the disordered harmonic chain, Prog. Theor. Phys. Suppl. **45**, 56 (1970).

[28] L. Zhang, J. Thingna, D. He, J.-S. Wang, and B. Li, Nonlinearity enhanced interfacial thermal conductance and rectification, Europhys. Lett. **103**, 64002 (2013).

[29] H. Koh, S. Chiashi, J. Shiomi, and S. Maruyama, Heat diffusion-related damping process in a highly precise coarse-grained model for nonlinear motion of SWCNT, Sci. Rep. **11**, 563 (2021).

[30] S. Hu, S. Ju, C. Shao, J. Guo, B. Xu, M. Ohnishi, and J. Shiomi, Ultimate impedance of coherent heat conduction in van der Waals graphene-MoS_2-heterostructures, Mater. Today Phys. **16**, 100324 (2021).

[31] H. A. Lorentz, The motion of electrons in metallic bodies: 1, 2, 3, Proc. K. Ned. Akad. Wet. **7**, 438 (1905).

[32] D. Alonso, R. Artuso, G. Casati, and I. Guarneri, Heat Conductivity and Dynamical Instability, Phys. Rev. Lett. **82**, 1859 (1999).

[33] G. Casati, C. Mejía-Monasterio, and T. Prosen, Magnetically Induced Thermal Rectification, Phys. Rev. Lett. **98**, 104302 (2007).

[34] B. Li, G. Casati, and J. Wang, Heat conductivity in linear mixing systems, Phys. Rev. E **67**, 021204 (2003).

[35] E. T. Swartz and R. O. Pohl, Thermal boundary resistance, Rev. Mod. Phys. **61**, 605 (1989).

[36] D. Ma and L. Zhang, Enhancement of interface thermal conductance between Cr–Ni alloy and dielectric via Cu nano-interlayer, J. Phys.: Condens. Matter **32**, 425001 (2020).

[37] J.-S. Wang, J. Wang, and J. Lü, Quantum thermal transport in nanostructures, Eur. Phys. J. B **62**, 381 (2008).

[38] N. Li and B. Li, Temperature dependence of thermal conductivity in 1D nonlinear lattices, Europhys. Lett. **78**, 34001 (2007).

[39] J. A. Thomas, J. E. Turney, R. M. Iutzi, C. H. Amon, and A. J. H. McGaughey, Predicting phonon dispersion relations and lifetimes from the spectral energy density, Phys. Rev. B **81**, 081411(R) (2010).

[40] J. Zhu, Y. Liu, and D. He, Effects of interplay between disorder and anharmonicity on heat conduction, Phys. Rev. E **103**, 062121 (2021).

[41] A. S. Pikovsky and D. L. Shepelyansky, Destruction of Anderson Localization by a Weak Nonlinearity, Phys. Rev. Lett. **100**, 094101 (2008).

[42] Z. Wang, W. Fu, Y. Zhang, and H. Zhao, Wave-Turbulence Origin of the Instability of Anderson Localization against Many-Body Interactions, Phys. Rev. Lett. **124**, 186401 (2020).

[43] M. V. Ivanchenko, T. V. Laptyeva, and S. Flach, Anderson Localization or Nonlinear Waves: A Matter of Probability, Phys. Rev. Lett. **107**, 240602 (2011).

[44] Z. Zhang, Y. Ouyang, Y. Cheng, J. Chen, N. Li, and G. Zhang, Size-dependent phononic thermal transport in low-dimensional nanomaterials, Phys. Rep. **860**, 1 (2020).